Received: 19 March 2020 | Revised: 16 September 2020 | Accepted: 19 September 2020

DOI: 10.1002/ima.22501

WILEY

RESEARCH ARTICLE

Detection of pneumonia in chest X-ray images by using 2D discrete wavelet feature extraction with random forest

Abdurrahim Akgundogdu

Electrical and Electronics Engineering Department, Istanbul University-Cerrahpasa, Istanbul, Turkey

Correspondence
Abdurrahim Akgundogdu, Electrical and Electronics Engineering Department, Istanbul University-Cerrahpasa, Istanbul, Turkey.
Email: akgundog@istanbul.edu.tr

Funding information
Scientific Research Projects Coordination Unit of Istanbul University-Cerrahpasa, Grant/Award Number: 23444

Abstract

Pneumonia is one of the most common and fatal diseases in the world. Early diagnosis and treatment are important factors in reducing mortality caused by the aforementioned disease. One of the most important and common techniques to diagnose pneumonia disease is the X-ray images. By evaluating these images, various machine-learning methods are used for accuracy in diagnosis. The presented study in this article utilizes machine-learning techniques to evaluate these X-ray images. The diagnosis of pediatric pneumonia is classified with a proposed machine learning method by using the chest X-ray images. The proposed system firstly utilizes a two-dimensional discrete wavelet transform to extract features from images. The features obtained from the wavelet method are labeled as normal and pneumonia and applied to the classifier for classification. Besides, Random Forest algorithm is used for the classification technique of 5856 X-ray images. A 10-fold cross-validation method is used to evaluate the success of the proposed method and to ensure that the system avoided overfitting. By using various machine learning algorithms, simulation results reveal that the Random Forest method is proposed and it gives successful results. Results also show that, at the end of the training and validation process, the proposed method achieves higher success with an accuracy of 97.11%.

KEYWORDS

image classification, machine learning, pneumonia, random forest, wavelet

1 | INTRODUCTION

Pneumonia is a fatal disease in generally underdeveloped countries, elderly communities, and infants.[1] Pneumonia, which influences 450 million people worldwide, affects infected lungs and alveoli and causes breath difficulties.[2] According to the World Health Organization (WHO), the pneumonia is estimated to cause the death of about 2 million children under the age of 5 each year.[3] WHO also reports that almost all (95%) cases of childhood pneumonia occur in developing countries, particularly in Southeast Asia and Africa. The difference between normal and pneumonia-infected alveoli is shown in Figure 1A.[4] The alveoli affected by pneumonia are filled with fluid and fewer blood cells, while healthy alveoli can hold enough air to perform normal functions. Although pneumonia is caused by a variety of microbes, it is usually caused by bacteria or viruses in the breathing air. Often, the body can fight off these germs that prevent it from spreading to the lungs. But sometimes the body's immune system is not strong.[2] Also, bacterial and viral pathogens require different forms of treatment.[5]

The diagnosis of pneumonia includes some processes such as chest X-ray analysis and physical examination. This is because a timely and accurate diagnosis is important. A radiographic image is an important diagnostic

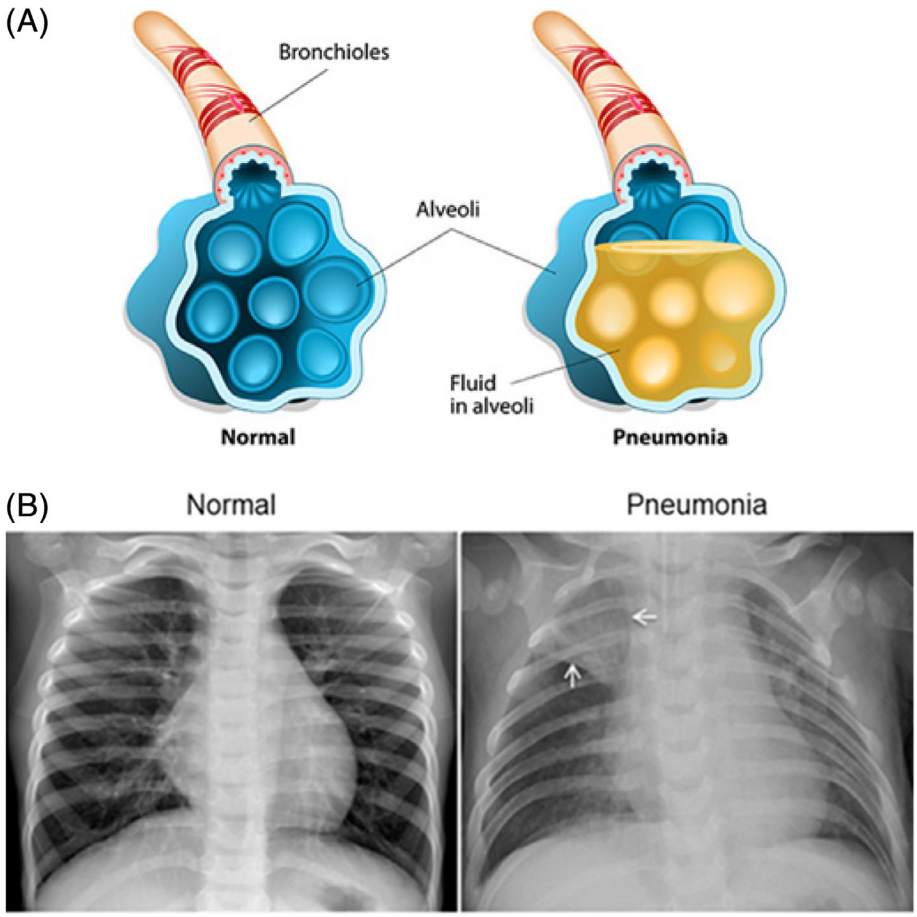

FIGURE 1 The diagram of pneumonia effects, A[4] and the example of chest X-ray in patients with pneumonia, B[6] [Color figure can be viewed at wileyonlinelibrary.com]

tool because of the chest X-rays can help to identify differences between different types of pneumonia. Figure 1B shows the chest X-rays of pneumonia and normal patients.

In the literature, the use of artificial intelligence for rapid and highly accurate interpretation of chest X-ray image analysis is becoming widespread.[7,8] Machine learning (ML), one of the artificial intelligence methods, learns to use chest X-ray images, and utilizes this knowledge to classify new images.[9-11] The aim of developing this model is to enable doctors to make a quick and almost accurate diagnosis and to provide more research and more time for patients in need.

The presented study in this article aims to develop a successful machine-learning model by using lung X-ray images and identify the methods and tools used. In this article, a total of 5856 chest X-ray images of 1583 normal and 4273 cases of pneumonia are examined. In the first stage of this study, which consists of two stages, attributes are extracted from the images. The classification process by using these attributes is performed in the second stage. Two Dimensional Discrete Wavelet method (2D DWT) is used for extracting attributes from images.[12-14] For the classification, Random Forest (RF)[15] method which is a well-known ML method is used. Different ML methods are also utilized in the process and it is evaluated that the most successful results are obtained from the RF method. The training data were used to determine the optimum RF classification model by verifying the different parameters and the feature significance was calculated for the best result.

In recent years, researchers have proposed different machine learning-based solutions for various medical issues. For instance, Ronneberger et al[16] utilized the CNN and data augmentation technique, and achieved successful results, with training on a small sample of images. Ke et al[17] used the spatial distribution of hue, saturation, and brightness techniques in the X-ray images as image descriptors and an ANN with heuristic algorithms to identify unhealthy lung tissues. Xu et al[18] planned a hierarchical CNN CXNet-m1, which utilized a novel sin-loss loss function to learn from misclassified and indistinguishable images for inconsistency identification on the chest X-rays. Jaiswal et al[19] used Mask-RCNN, a deep neural network, which utilizes both global and local features for pulmonary image segmentation combined with image augmentation, alongside with dropout and L2 regularization, for pneumonia identification. Wozniak and

Połap simulated the medical X-ray image inspection process to show the location of possibility of infected tissues.[20] Nobrega et al investigated the execution of deep transfer learning from non-medical images on lung nodule malignancy classification tasks to improve lung nodule malignancy classification.[21] They compared the ResNet50 feature extractor combined with the SVM RBF classifier for recognition of the malignancy of a lung nodule. Chouhan et al[22] propose a novel deep learning framework for the detection of pneumonia utilizing the concept of transfer learning. Their study aims to simplify the pneumonia detection process for specialists as well as for beginners. Wang et al[23] contributed by proposing a new dataset called ChestX-ray8 that contains images of distinctive 32 717 patients, having 108 948 frontal X-ray images. They accomplished promising results using a deep CNN. Afterward, Recurrent Neural Network (RNN) method is used in the study conducted by Yao et al.[24] They presented and evaluated a partial solution by using Long-short Term Memory Networks (LSTM) to leverage interdependencies among target labels in predicting 14 pathologic patterns from the chest X-rays images. Rajpurkar et al tried to increase the success rates by using the deep learning in their studies.[25] Kermany classified viral and bacterial with Image-Based Deep Learning.[6]

The rest of this article is organized as follows. Section 2 describes the materials and methods of the proposed system, 2D DWT, RF, and assessment of methods. Results, comparisons, and discussion are presented in Section 3. Finally, Section 4 concludes the article.

2 | MATERIALS AND METHODS

In this work, 5856 chest X-ray images are used as a dataset.[26] The dataset includes 4273 cases of pneumonia and 1583 normal case. In this model, normal cases are labeled as "normal" and pneumonia cases represented as "pneumonia". The proposed method consists of two steps: The first step is feature extraction by using 2D DWT and the second step is the classification by using RF. The block diagram of the proposed scheme is presented in Figure 2. As shown in Figure 2, the initial approximate coefficients are subtracted from X-ray images by using level-1 2D DWT. Finally, the features are classified by the RF classifier. Algorithm 1 gives an overview of the proposed approach.

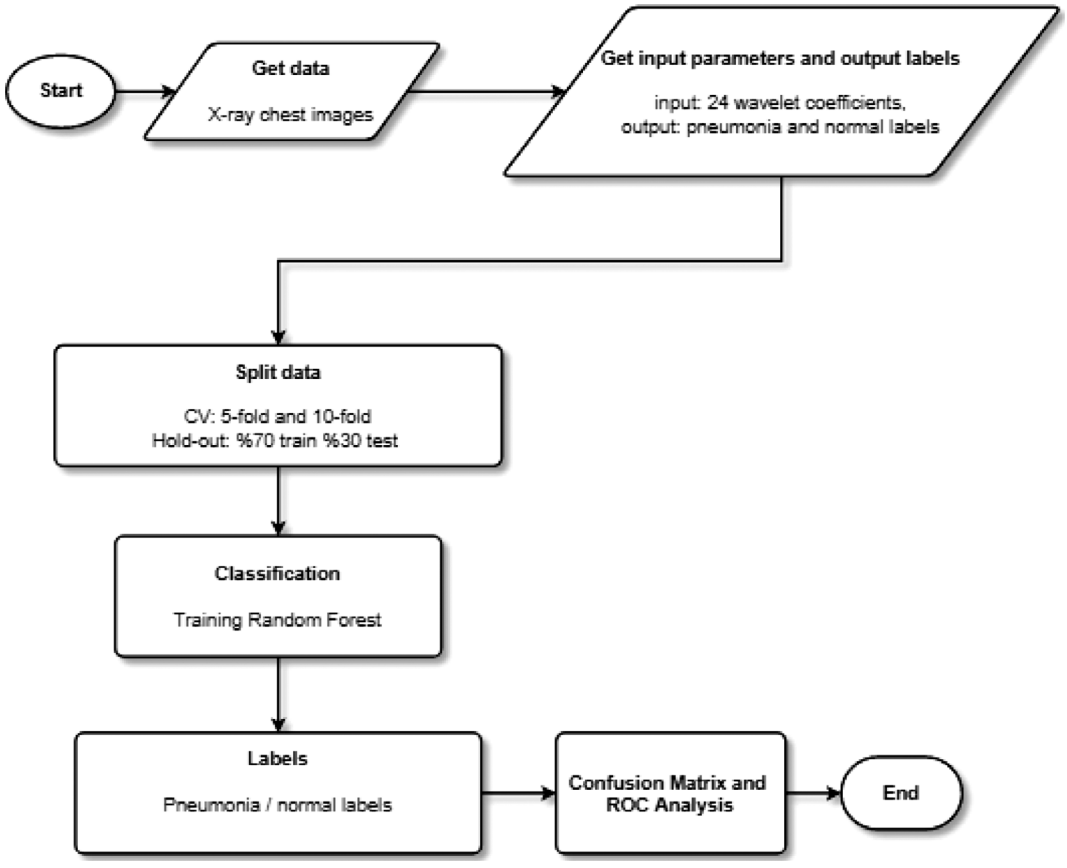

FIGURE 2 Flowchart for the proposed pneumonia disease classification method

Algorithm 1 Proposed approach.

1: —Feature extraction—
2: **for** i = 1:1:5856 **do** read all images I_i
3: —Calculate Wavelet coefficients—
4: Calculate 6 approximation wavelet coefficients
5: Calculate 6 vertical wavelet coefficients
6: Calculate 6 horizontal wavelet coefficients
7: Calculate 6 diagonal wavelet coefficients
8: Save all 24 wavelet coefficients as input parameters and label pneumonia or normal case
9: **end for**
10: —Classification—
11: Read the input parameters vs output labels
12: Train and validate with Random Forest
13: Save Random Forest trees t_1, t_2, ... 327
14: Classify using Random Forest

2.1 | Feature extraction based on 2D discrete wavelet transform

Wavelet analysis is a mathematical tool used to extract image properties and it provides successful results in many image analysis studies.[14] The wavelet decomposition of a signal helps to extract different information of the main signal, such as high frequency or low frequency segments. This conversion is very useful for analyzing the signal or image at different scales or resolutions and provides highly successful results for classification. Figure 3 shows a schematic diagram of 2D DWT. In images, DWT is applied to each size separately.

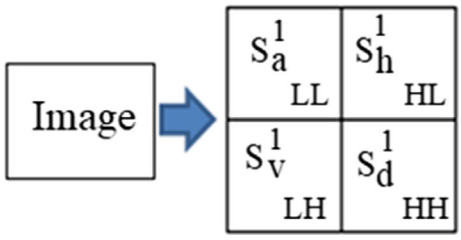

FIGURE 3 Schematic diagram of 2D DWT (LL: low–low, LH: low–high, HL: high–low, HH: high–high) [Color figure can be viewed at wileyonlinelibrary.com]

The wavelet transform of a 2D image $f(x,y)$ is characterized as the connection between the image and a family of wavelet functions $\phi_{s,t}(x, y)$

$$W_{f(s,t;x,y)} = \int\int f(x,y)\phi_{s,t(x,y)}dxdy \quad (1)$$

Wavelets $\phi_{s,t}(x,y)$ are generated from a mother wavelet function $\phi(x, y)$ as follows:

$$\phi_{s,t}(x,y) = \frac{1}{s}\Phi\left(\frac{(x-t_x)}{s}, \frac{(y-t_y)}{s}\right) \quad (2)$$

where s is the scale parameter, t_x, and t_y are the translation parameters in the x-axis and y-axis.[27] There are several types of wavelets that have become widespread throughout the development of wavelet analysis. One of the effective and simple wavelet techniques is the Daubechies 4 wavelet, which is frequently used for various types of applications.[28,29] The technique is very fast and can be used to extract basic structural information from an image. In this study, 1-level Daubechies-4 DWT types are used. By application of wavelet transform, four subgroups are obtained (LL: low-low, LH: low-high, HL: high-low, HH: high-high) such as:

$$S^1 = S_a^1 + S_v^1 + S_h^1 + S_d^1 \quad (3)$$

The input image S^1 is decomposed into a first-level S_a^1 (approximation component, LL) and S_v^1, S_h^1, S_d^1 (detail components; vertical (LH), horizontal (HL), and diagonal (HH)). Here, pneumonia person's X-ray image has been decomposed to 1-level using the DWT approach using Matlab wavelet analysis.[30] Figure 4 shows that the images vary in vertical, horizontal, and diagonal states.

At the output of DWT block, 24 statistical features of each image are extracted as minimum (min), maximum (max), mean, SD (first moment, std), variance (second moment, var), and third moment values of approximation, vertical, horizontal, and diagonal of wavelet subbands are shown in Figure 5.

2.2 | Classification based on random forests

In recent years, algorithms based on decision trees and combining most of these trees have gained importance. The most prominent of these methods is the RF method introduced by Breiman.[15] In the RF method, the results of multiple classifiers are combined and a single decision is made on behalf of the community, thus making more reliable estimates. The RF method is a forest classifier consisting of a large number of decision trees and can be

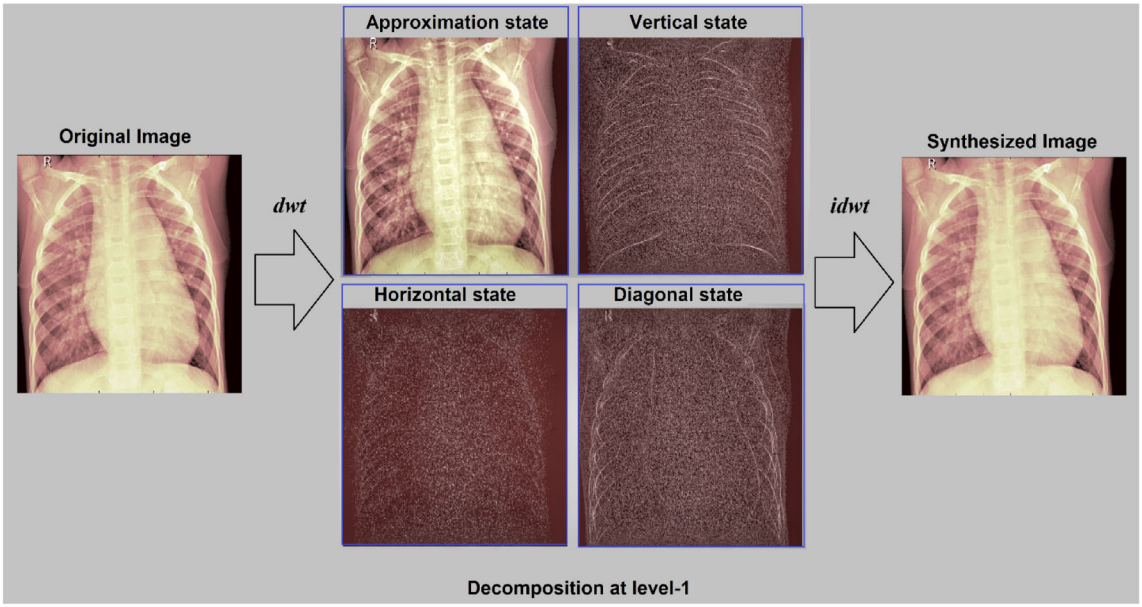

FIGURE 4 Pneumonia X-ray image and its 2D wavelet coefficients at level-1 decomposition [Color figure can be viewed at wileyonlinelibrary.com]

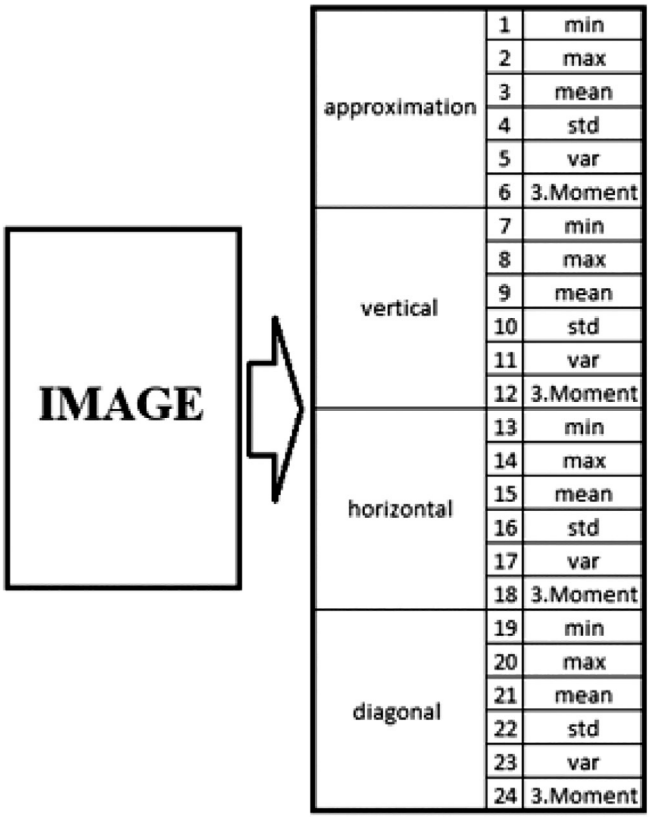

FIGURE 5 Feature extraction block (24 statistical features of each image)

used for classification or regression trees. Each decision tree in the forest is created by selecting a sample from the original data set with the bootstrap technique and selecting a specified number of random variables from all variables in each decision node. In this method, trees are created and not pruned.

An RF versatile classifier consists of a series of trees in which each tree is grown using a kind of randomization method. The classification decision is made by taking the average of the class assignment possibilities calculated by all trees produced. A new unlabeled data entry is evaluated against all decision trees created in the community and each tree votes for class membership. The membership class with the most votes will finally be the chosen one.

The steps of the RF classifier are as follows:

- The number of decision trees to be created by using the attributes of the data set (t) is determined.
- At each node in the trees, random m variables are selected and the best branch is determined.
- The best branch is divided into two sub-branches again and the tree branching process ends until the gini[31] index reaches zero.

$$Gini\left(S_M^L\right) = 1 - \sum_{i=1}^{K} p_i^2 \tag{4}$$

where S_M^L refers to the selected subset consisting of L instances and M features, p_i the frequency of samples of the i_{th} category, and k is the number of categories.

- The class that receives the most votes among the individual estimates made by n decision tree is chosen as the final decision estimate Figure 6[32] shows the general structure of the RF classifier.

After all, trees have been built, an entry vector x is classified by taking the majority of the votes cast by all trees in the community. In this article, the RF technique is used to classify chest X-ray images. Results show that the RF technique provides higher classification performance on all data sets.

2.3 | Assessment and comparison of model performance

Cross-validation (CV) is a general method for assessing the performance of learning methods for optimal performance.[33] The performance of the RF algorithm was assessed using 10-fold CV. In this study, there a total number of 5856 X-ray images are used in the RF analysis, where each fold contains 10 groups. For each of 10-folds of the original data, a model was constructed by using cases in the remaining nine folds and validated on cases in the 10th fold. As an example, an illustration of the 10-folds scheme is given in Figure 7.

For computing the loss function with index t, the classification error is:

$$\epsilon_t = \sum_{n=1}^{N} d_n^t I(y_n \neq h_t(x_n)) \tag{5}$$

where x_n is a vector of predictor values for observation n term, y_n is the true class label (normal case), h_t is the prediction of learner with index t, I term is the indicator function and d_n^t is the weight of observation n at step t.

2.4 | Diagnostic accuracy and receiver operating characteristics (ROC) analysis

Diagnostic accuracy addresses the agreement between a proposed test and a reference standard for the ability to define a target condition. Equations for calculating accuracy, sensitivity, specificity, F-score, and kappa values are shown in (6), (7), (8), (9), (10), respectively.

$$\text{Accuracy} = \frac{TP + TN}{TP + TN + FP + FN} \tag{6}$$

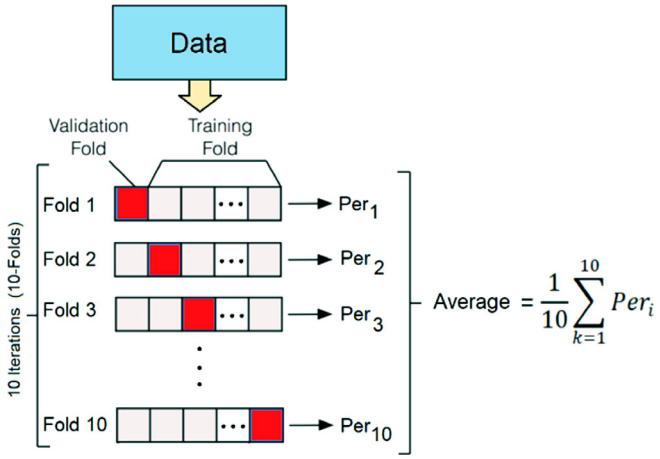

FIGURE 7 Illustration of the 10-fold CV method [Color figure can be viewed at wileyonlinelibrary.com]

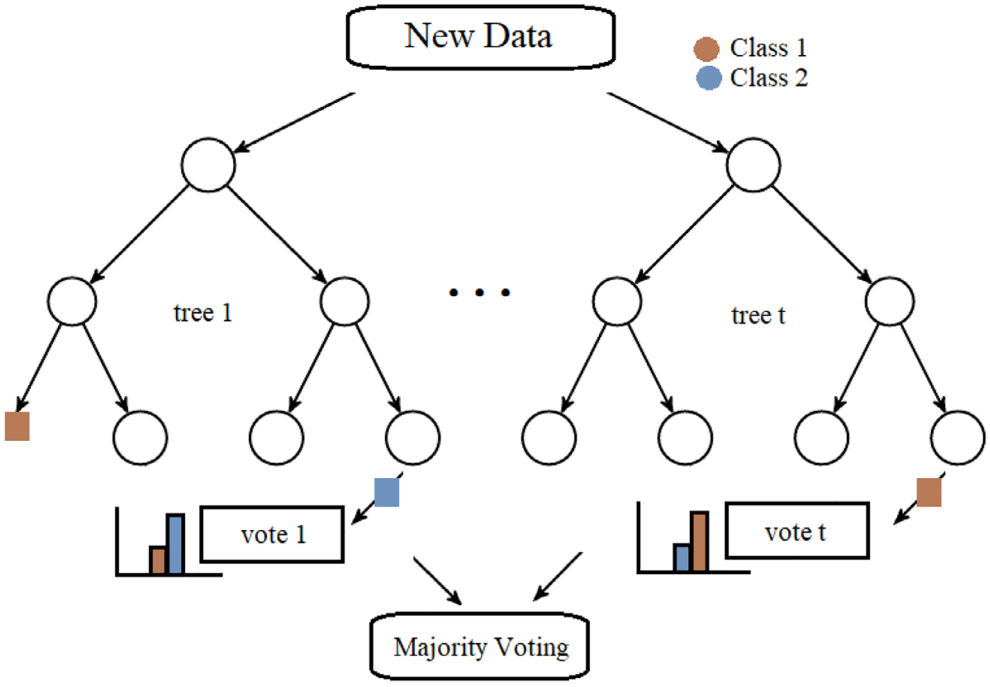

FIGURE 6 The scheme of Random Forests classifier [Color figure can be viewed at wileyonlinelibrary.com]

$$\text{Sensitivity (recall)} = \frac{TP}{TP + FN} \tag{7}$$

$$\text{Specificity} = \frac{TN}{TN + FP} \tag{8}$$

$$F - \text{score} = \frac{2TP}{2TP + FP + FN} \tag{9}$$

$$\text{Kappa statistic} = \frac{Po - Pe}{1 - Pe} \tag{10}$$

where *TP* (True Positive) represents the correctly classified positive cases, *TN* (True Negative) denotes correctly classified negative cases, *FN* (False Negative) is the incorrectly classified positive cases and *FP* (False Positive) means incorrectly classified negative cases, *Po* is the observed agreement, and *Pe* is the expected agreement. *Po* and *Pe* are formulated below:

$$Po = \frac{TP + TN}{TP + TN + FP + FN} \tag{11}$$

$$Pe = \frac{(TP + FN)(TP + FP) + (FP + TN)(FN + TN)}{(TP + TN + FP + FN)^2} \tag{12}$$

The confusion matrix is a way to show the performance of a classifier for classification tasks. This square matrix consists of columns and rows that list the number of samples as "Positive" and "Negative" ratios. The definitions with respect to the confusion matrix are summarized in Table 1.

ROC curves provide an effective tool for analyzing features of normal and diseased individuals. All possible combinations of TP and FP create a ROC area. A TP and an FP together determine a single point in the ROC[34] space, and the position of a point in the ROC space indicates the balance between sensitivity and specificity, that is, an increase in sensitivity is accompanied by a decrease in specificity.

TABLE 1 An example of a 2 × 2 confusion matrix for two labels

	Predicted values	
Actual values	**Positive**	**Negative**
Positive	True positive (TP)	False negative (FN)
Negative	False positive (FP)	True negative (TN)

TABLE 2 Comparison of MLs with 10-fold cross-validation

Classifier	**Effective parameters**	**Sensitivity (%)**	**Specificity (%)**	**Accuracy (%)**	***F*-score**	**Kappa statistic**	**ROC area (AUC)**	**Time is taken to build the model (seconds)**
ANN	Hidden Neuron:13 Learning Rate:0.3 Activation Function: Unipolar Sigmoid	90.02	98.01	95.85	0.9214	0.8933	0.982	44.82
K-NN	Distance: Euclidean Number of Neighborhood: 3	89.13	96.44	94.50	0.8976	0.8600	0.965	14.2
SVM	C:2 Kernel: Poly Kernel	85.22	94.62	93.41	0.8748	0.8301	0.908	8.9
RF (proposed model)	Number of Trees: 327 Number of Iteration:100	91.79	99.09	97.11	0.9804	0.9255	0.99	16.9

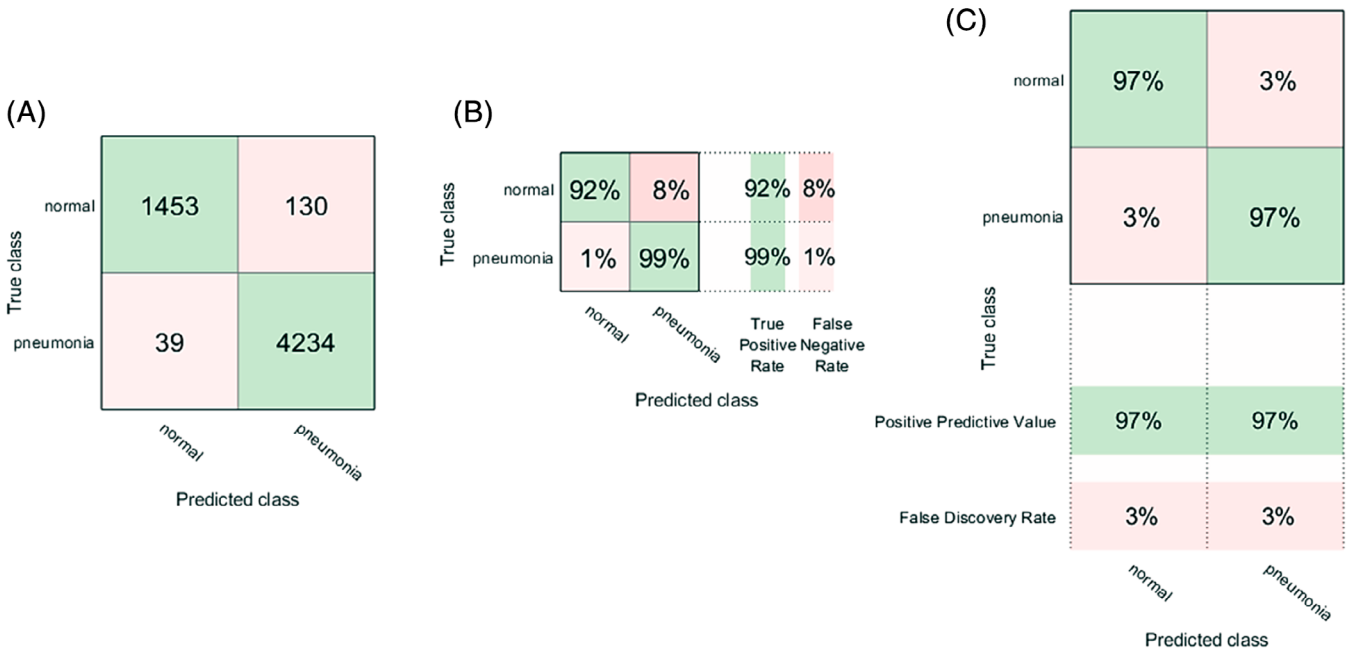

FIGURE 8 Confusion matrix for the RF classifier by using 10-fold cross validation, A, Number of observations, B, True positive rates vs false negative rates, and C, Positive predictive values vs false discovery rates) [Color figure can be viewed at wileyonlinelibrary.com]

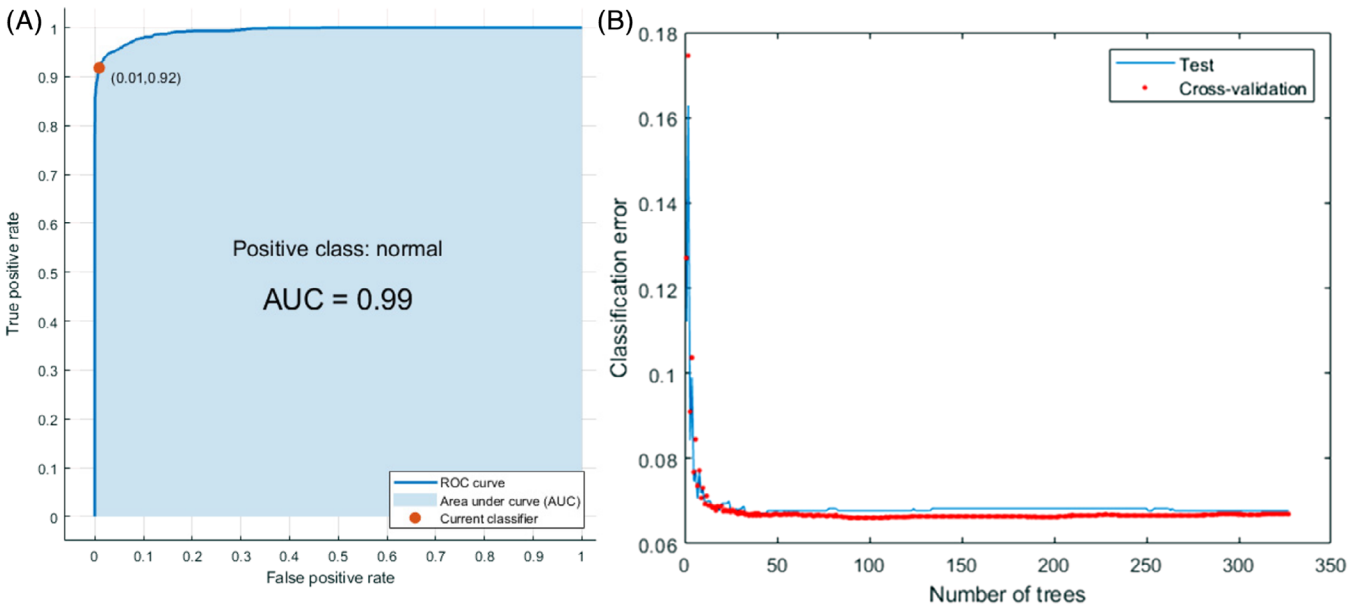

FIGURE 9 For 10-fold CV; ROC curve used to evaluate the performance of the Random Forests method that is drawn from two variables: false positive rate and true positive rate, A, and classification error vs the number of trees, B [Color figure can be viewed at wileyonlinelibrary.com]

3 | RESULTS AND DISCUSSION

In this section, 5856 X-ray images, which are verified by specialist doctors, are used as a dataset. These images contain 1583 normal and 4273 pneumonia cases. Before the training and testing process, the wavelet feature extraction method is used for the acquisition of the input parameters. According to the classification results shown in Table 2, the classification accuracy of the proposed method which is 97.11%, specificity 99.09%, sensitivity 91.79%, and area under the curve (AUC) value is 0.99 for 10-fold CV. The performance measures are calculated based on the confusion matrix, which is presented in Figure 8. Interpreting Figure 8, accuracy is the ratio of

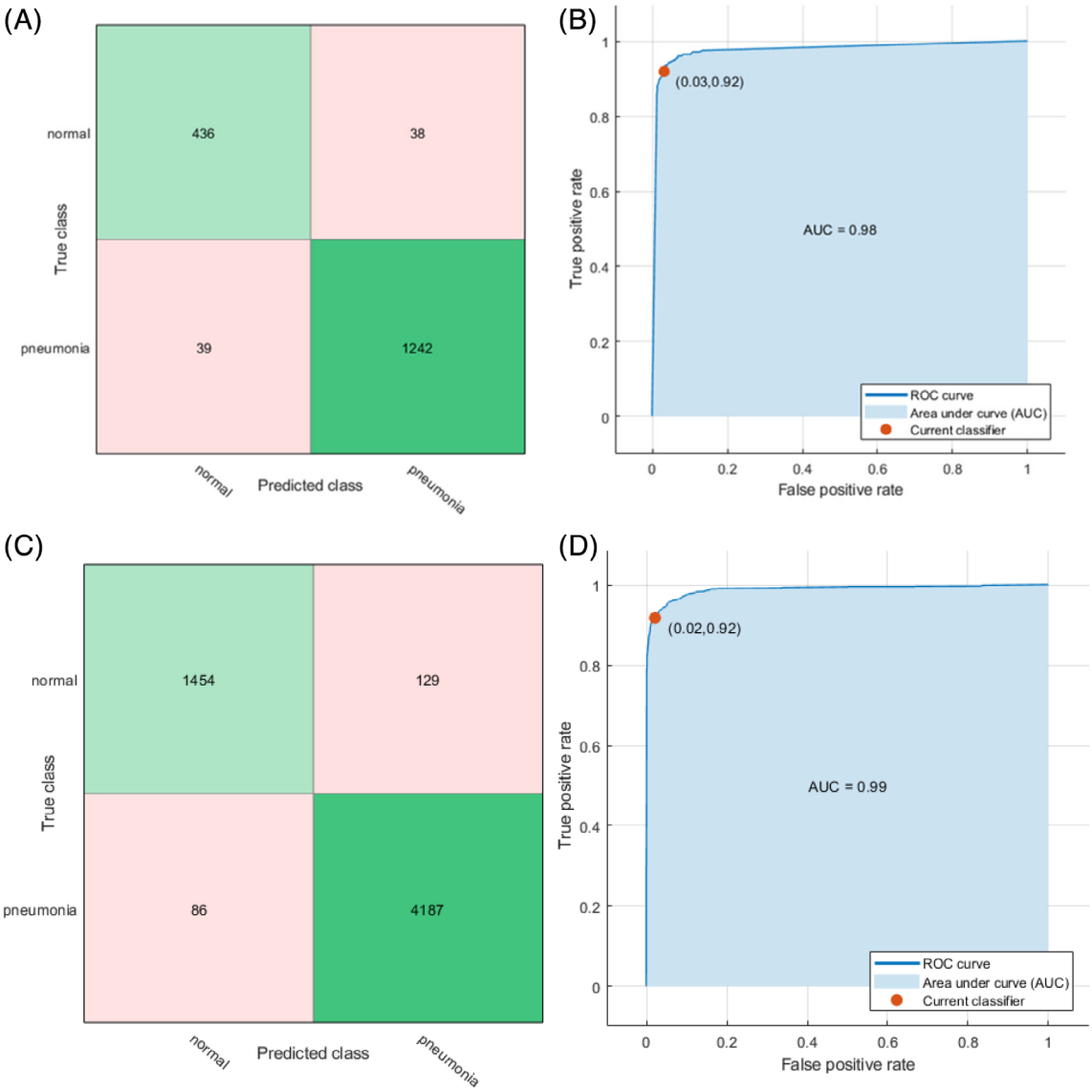

FIGURE 10 Confusion matrices and ROC curves of hold-out, A,B, and 5-fold CV, C,D, results [Color figure can be viewed at wileyonlinelibrary.com]

the number of correctly classified samples to the total number of samples, sensitivity is the ratio of the number of correctly classified positive samples to the total number of positive samples and specificity is equal to the true negative number divided by the sum of true negatives and false positive numbers.

To better evaluate the performance of the proposed method, the ROC curve, and the AUC for detection of normal from pneumonia have been plotted and shown in Figure 9A. Figure 9B shows the loss function of the classification error vs trees. The error tends to decrease with testing and cross-validation. To avoid an over-fitting problem and to make the classifier generalize to the dataset, the 10-fold CV method is employed for the dataset. The CV steps are presented in Algorithm 2.

Algorithm 2 Training and validation.

1: —Cross-Validation—
2: Randomly split all dataset into $k = 10$ folds
3: For each k-fold in the dataset, build k-1 folds of the dataset
4: Save the error on each of the predictions
5: Repeat this until each of the k-folds has served as the validation set
6: Save the average of k errors
7: Calculate the performance

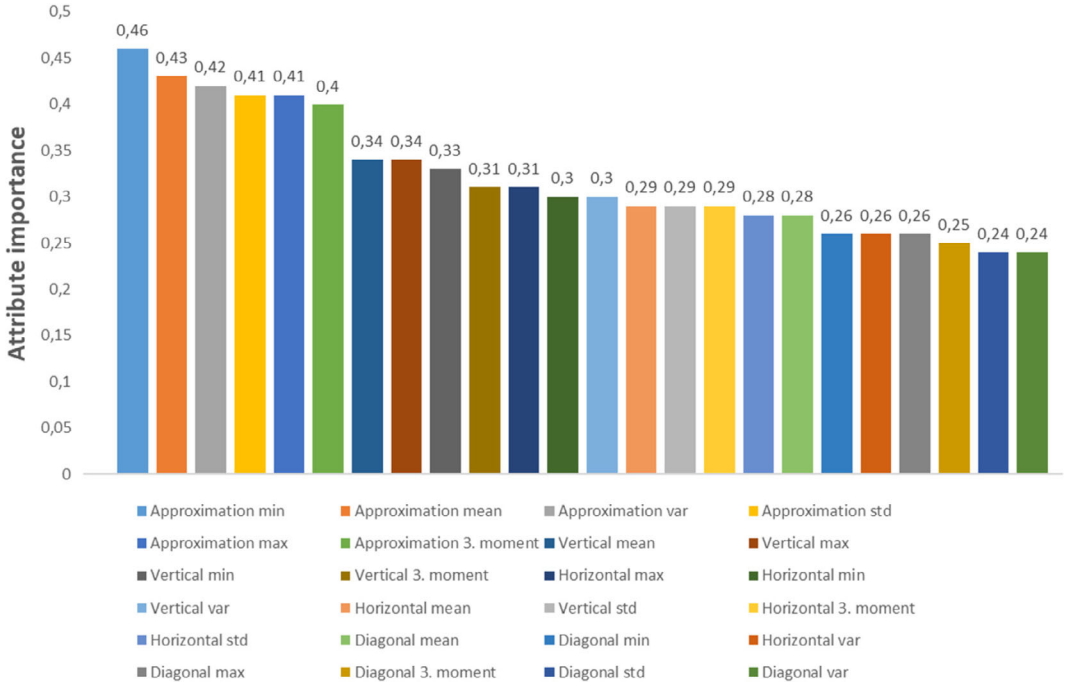

FIGURE 11 Attribute importance based on average impurity decrease in RF [Color figure can be viewed at wileyonlinelibrary.com]

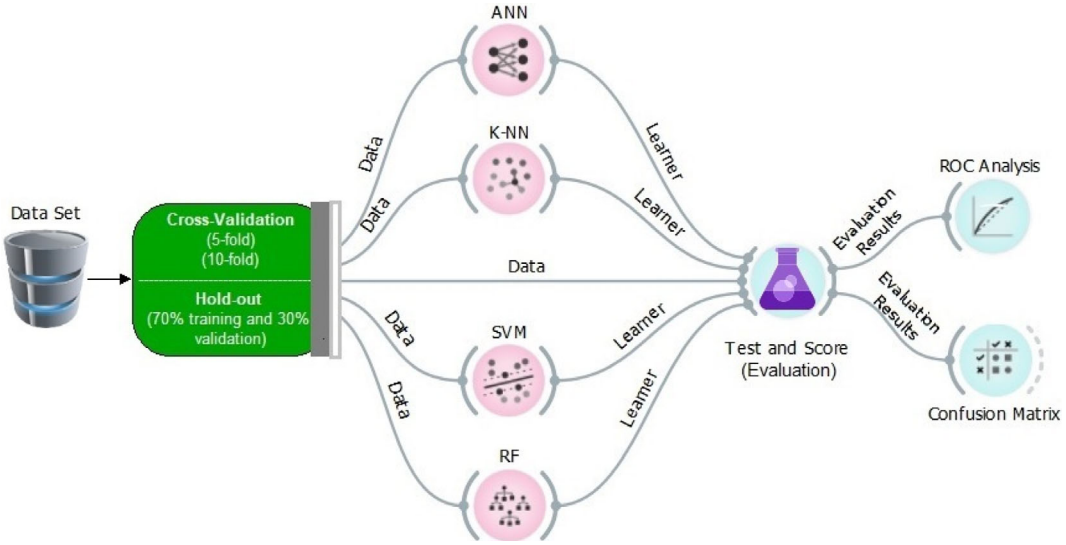

FIGURE 12 Knowledge flow of different ML models [Color figure can be viewed at wileyonlinelibrary.com]

Implementation: The RF algorithm is utilized in this experiment, including the 2D wavelet method is also performed by using the Matlab program on a personal computer (Intel Core i5, 4 Gb Ram, 1 Gb Nvidia Graphic card). The time duration is also represented in Table 2.

The data set was divided into different sections and validation was done to avoid the over-fitting problems. 5-fold CV and hold-out (70% training and 30% validation) results are shown in Figure 10. Figure 10A,B shows the confusion matrix and ROC curve of hold-out results. Likewise, Figure 10C,D presents the confusion matrix and ROC curve of 5-fold CV results respectively.

The *F*-score and kappa values obtained after 10-fold CV are shown in Table 2. Here, the *F*-score value is 0.9804 and the kappa value is 0.9255, respectively.

In this study, the feature significance was calculated according to the average impurity reduction[35] for the optimum RF parameters selected and is shown in Figure 11. In detail, all attributes have very close importance to each other. But approximation minimum has

TABLE 3 Summary of related studies

Studies	Methods	AUC
Kermany[6]	Image-Based Deep Learning	0.968
Wang et al[16]	ResNet-50	0.633
Yao et al[17]	LSTM	0.713
Rajpurkar et al[18]	CheXNet	0.768
Chen et al[36]	DualCheXNet	0.823
Ayan and Unver[37]	Vgg16	0.87
Narayanan et al[38]	AlexNet, ResNet, VGG16 and Inception-v3	0.996
This study	2DW RF	0.99

been seen as the most important attributes which have a 0.46 impurity decrease.

In this study, chest X-ray images were classified by combining 2D wavelet and RF models. After obtaining the attributes by 2D wavelet method, different ML models and the RF model were compared. The 24 features, which are used as inputs, with a target, as an output vector are sent to the RF classifier. To find the most suitable parameters of RF, various parameters to be selected for each node of the tree are determined at the end of the tests. The proposed system works well for a dataset using 24 feature parameters. The performance metrics of the RF classifier with other classifiers, namely, KNN (K-Nearest Neighborhood), ANN (Artificial Neural Network), and SVM (Support Vector Machine), are calculated during the run of the CV procedure, which is listed in Table 2. An experiment has been carried out to estimate the optimal value of the parameters used in other classifiers and finally, the values with the lowest error rate are selected to train these classifiers. As can be seen from Table 2, the RF method has achieved the most successful results with 327 trees and 100 iterations. Figure 12 shows a block diagram of the different ML models compared in this study.

AUC values obtained in previous studies for the classification of pneumonia X-ray images are shown in Table 3. As can be seen from Table 3, the proposed 2DW-RF model gives the high AUC value. The proposed method reaches the AUC score for 5856 X-ray images is 0.99 with 97.11 accuracies.

4 | CONCLUSIONS

In this study, a two-stage approach to chest X-ray classification has proposed and performance on the diagnosis of pneumonia disease was calculated. Five thousand eight hundred and fifty-six chest X-ray images are utilized, 2D DWT and RF methods are conducted for successful classification. These images are chest X-ray images of normal and pneumonia patients. In this work, attributes are extracted from the images by using the wavelet method and the obtained attributes are used as input for the RF method. In this article, which used different machine learning methods, the RF method was found to be very successful according to the classification of pneumonia cases. The results have shown that the proposed 2D DWT and RF method performs better than other comparable ML methods. The proposed method achieves 97.11% accuracy on chest X-ray images. In case the chest X-ray images are examined; while classifying those with normal conditions and cases of pneumonia; for 10-fold CV: 130 out of 4234 pneumonia cases were misdiagnosed, 39 samples were misdiagnosed for 1453 normal cases. In reference to results, the success rate obtained in the diagnosis of pneumonia patients is higher. In the proposed method, when wavelet level-1 and RF method are used together, it is much faster than deep learning methods and gives very high successful results. Here, it is necessary to prevent the RF from getting overfitting instead of learning. For this reason, whether the proposed system is more compatible or not was checked with 5-fold, 10-fold CV and 70% to 30% hold out methods. In future studies, performance evaluation of the system can be made by using deep learning methods.

ACKNOWLEDGMENT

This study was funded by Scientific Research Projects Coordination Unit of Istanbul University-Cerrahpasa. Project numbers: 23444.

CONFLICT OF INTEREST

The author declares that he has no conflict of interest.

RESEARCH WITH ANIMAL AND HUMAN PARTICIPANTS

This article does not contain any studies with human participants or animals performed by the author.

INFORMED CONSENT

No informed consent was required.

ORCID

Abdurrahim Akgundogdu https://orcid.org/0000-0001-8113-0277

REFERENCES

1. Kabra SK, Lodha R, Pandey RM. Antibiotics for community-acquired pneumonia in children. *Cochrane Database Syst Rev*. 2006;3:CD004874.
2. Mayo Clinic. *Pneumonia-Symptoms and Causes*. 2018 https://www.mayoclinic.org/diseases-conditions/pneumonia/symptoms-causes/syc-20354204/. Accessed September 26, 2018.
3. Rudan I, Boschi-Pinto C, Biloglav Z, Mulholland K, Campbell H. Epidemiology and etiology of childhood pneumonia. *Bull World Health Organ*. 2008;86:408-416.

4. Pneumonia Ausmed. *Pneumonia Symptoms. Signs and Treatment*. https://www.ausmed.com/cpd/articles/pneumonia/. Accessed July 3, 2019.
5. Mcluckie A. *Respiratory Disease and its Management*. New York: Springer; 2009.
6. Kermany DS, Goldbaum M, Cai W, et al. Identifying medical diagnoses and treatable diseases by image-based deep learning. *Cell*. 2008;172:1122-1131.
7. Zhang J, Gajjala S, Agrawal P, et al. Fully automated echocardiogram interpretation in clinical practice. *Circulation*. 2018; 138:1623-1635.
8. Rogers TW, Jaccard N, Morton EJ, Griffin LD. Automated X-ray image analysis for cargo security: critical review and future promise. *J Xray Sci Technol*. 2016;25:1-24.
9. Komura D, Ishikawa S. Machine learning methods for histopathological image analysis. *Comput Struct Biotechnol J*. 2018; 16:34-42.
10. Erickson BJ, Korfiatis P, Akkus Z, Kline TL. Machine learning for medical imaging. *Radiographics*. 2017;37(2):505-515.
11. Zhou M, Scott J, Chaudhury B, et al. Radiomics in brain tumor: image assessment, quantitative feature descriptors, and machine-learning approaches. *Am J Neuroradiol*. 2018;39:208-216.
12. Lumini A, Nanni L, Brahnam S. Multilayer descriptors for medical image classification. *Comput Biol Med*. 2016;72:239-247.
13. Beura S, Majhi B, Dash R. Mammogram classification using two dimensional discrete wavelet transform and gray-level co-occurrence matrix for detection of breast cancer. *Neurocomputing*. 2015;154:1-14.
14. Chaplot S, Patnaik LM, Jagannathan NR. Classification magnetic resonance brain images using wavelets as input to support vector machine and neural network. *Biomed Signal Process Control*. 2006;1:86-92.
15. Breiman L. Random forests. *Mach Learn Springer*. 2001;45: 5-32.
16. Ronneberger O, Fischer P, Brox T, 2015. U-net: convolutional networks for biomedical image segmentation. *Proc Int Conf Medical Image Comput Comput-Assisted Intervention* 234–241.
17. Ke Q, Zhang J, Wei W, et al. A neuro-heuristic approach for recognition of lung diseases from X-ray images. *Expert Syst Appl*. 2019;126:218-232.
18. Xu S, Wu H, Bie R. CXNet-m1: anomaly detection on chest X-rays with image-based deep learning. *IEEE Access*. 2019;7:4466-4477.
19. Jaiswal AK, Tiwari P, Kumar S, Gupta D, Khanna A, Rodrigues JJPC. Identifying pneumonia in chest X-rays: a deep learning approach. *Meas J Int Meas Confed*. 2019;145:511-518.
20. Woźniak M, Połap D. Bio-inspired methods modeled for respiratory disease detection from medical images. *Swarm Evol Comput*. 2018;41:69-96.
21. da Nóbrega RVM, Rebouças Filho PP, Rodrigues MB, da Silva SP, Júnior CMD, de Albuquerque VHC. Lung nodüle malignancy classification in chest computed tomography images using transfer learning and convolutional neural networks. *Neural Comput Appl*. 2020;32:11065-11082.
22. Chouhan V, Singh SK, Khamparia A, et al. A novel transfer learning-based approach for pneumonia detection in chest X-ray images. *Appl Sci*. 2020;10:559.
23. Wang X, Peng Y, Lu L, Lu Z, Bagheri M, 2017. Summers, R.M.: Chestx-ray8: hospital-scale chest x-ray database and benchmarks on weakly-supervised classification and localization of common thorax diseases. *2017 IEEE Conference on Computer Vision and Pattern Recognition (CVPR)* 3462–3471.
24. Yao L, Poblenz E, Dagunts D, Covington B, Bernard D, Lyman K, 2017. Learning to diagnose from scratch by exploiting dependencies among labels. arXiv,1710.10501
25. Rajpurkar P, Irvin J, Zhu K, Yang B, Mehta H, Duan T et al (2017) CheXNet: radiologist-level pneumonia detection on chest X-rays with deep learning arXiv 1711.05225
26. Kermany D, Zhang K, Goldbaum M, 2018. Labeled optical coherence tomography (OCT) and chest X-Ray images for classification. Mendeley Data v2
27. Mallat S. A theory for multiresolution signal decomposition: the wavelet representation. *IEEE Trans Pattern Anal Mach Intell*. 1989;11:674-693.
28. Daubechies I. *Ten Lectures on Wavelets*. Philadelphia: SIAM; 1992.
29. Nayak DR, Dash R, Majhi B. Brain MR image classification using two-dimensional discrete wavelet transform and AdaBoost with random forests. *Neurocomputing*. 2016;177: 188-197.
30. MathWorks. *Matlab and Wavelet Toolbox 2013b*. Massachusetts, United States: The MathWorks Inc; 2013.
31. Pal M. Random forest classifier for remote sensing classification. *Int J Remote Sens*. 2005;26:217-222.
32. Belgiu M, Drăguţ L. Random forest in remote sensing: a review of applications and future directions. *ISPRS J Photogramm Remote Sens*. 2016;114:24-31.
33. Santos MS, Soares JP, Abreu PH, Araujo H, Santos J. Cross-validation for imbalanced datasets: avoiding overoptimistic and overfitting approaches. *IEEE Comput Intell Mag*. 2018;13:59-76.
34. Hanley JA, McNeil BJ. The meaning and use of the area under a receiver operating characteristic (ROC) curve. *Radiology*. 1982;143:29-36.
35. Louppe G, Wehenkel L, Sutera A, Geurts P. Understanding variable importances in forests of randomized trees. In: Burges CJC, Bottou L, Welling M, Ghahramani Z, Weinberger KQ (eds.), *Advances in Neural Information Processing Systems*. Red Hook, NY, USA: Curran Associates, Inc. 2013;26:431-439. http://papers.nips.cc/paper/4928-understanding-variable-importances-in-forests-of-randomized-trees.pdf.
36. Chen B, Li J, Guo X LG. DualCheXNet: dual asymmetric feature learning for thoracic disease classification in chest X-rays. *Biomed Signal Process Control*. 2019;53:101554.
37. Ayan E, Ünver HM, 2019. Diagnosis of pneumonia from chest X-ray images using deep learning. *2019 Scientific Meeting on Electrical-Electronics and Biomedical Engineering and Computer Science (EBBT)*. Istanbul, Turkey, 1–5.
38. Narayanan BN, Davuluru VSP, Hardie RC. Two-stage deep learning architecture for pneumonia detection and its diagnosis in chest radiographs. *Proc SPIE Med Imaging*. 2020;11318:1-10.

How to cite this article: Akgundogdu A. Detection of pneumonia in chest X-ray images by using 2D discrete wavelet feature extraction with random forest. *Int J Imaging Syst Technol*. 2020; 1–12. https://doi.org/10.1002/ima.22501